Stent Material Nitinol – Determination of Characteristics and Component Simulation Using the Finite Element Method

K. KOOP, D. LOOTZ, C. KRANZ, C. MOMMA, B. BECHER*, M. KIECKBUSCH
Institute for Implant Technology, Rostock-Warnemünde, Germany
*Institute for Biomedical Engineering, University of Rostock, Rostock, Germany

Summary

Intravascular scaffolding devices, known as stents, are in clinical use for the treatment of vessel stenoses. A stent is first compressed to a small diameter, then transferred to the stenosed part of the vessel by means of a catheter, and finally expanded to its nominal diameter. The expansion is effected either by a balloon or by a material-inherent ability to self-expansion. Self-expanding stents, which are being used increasingly often in the peripheral vessels, are preferably made of the shape-memory alloy Nitinol. In the first step, the goal of this investigation is to describe the properties of this material that are related to device construction, as well as to indicate possible means of thermo-mechanical treatments for the tailoring of material characteristics. Using these results, parameters are defined that lead to characteristics fulfilling the requirements to a stent material. In a second step, a material law is deduced from the material data that is suited for use within a Finite Element program. This method is validated by direct comparison to experimental results from tension tests. Finally, the enormous potential of this method is exemplified by presenting calculations of selected loading states of vascular stents.

Key Words

Stent, self-expanding stent, shape memory alloy, Nitinol, finite element analysis

Introduction

Nitinol (Nickel Titanium Naval Ordinance Laboratory), a binary alloy consisting of nickel and titanium, is the most commonly used shape-memory alloy in medicine due to its known biocompatibility. The principle behind these alloys was discovered and described in the 60's. The essential characteristics are the temperature-dependent shape-memory effect, and the superelasticity (especially the possible elastic strain of max. 8 %). The material characteristics are defined by the composition of the two alloy components, and can be adapted to the given requirements by choosing the appropriate heat treatment. This results in a multitude of interesting possibilities for application. However, because of the difficult requirements and the detailed knowledge of materials science required of the producer of the material, the use of the material has so far been limited to a few fields such as air or space travel, or medical technology. This is also because research, development, and manufacturing with Nitinol is very cost-intensive.

Many different shape memory alloys are used in industry, mainly based on Fe, Cu, or NiTi. In medical technology, the binary nickel-titanium alloy is the most common, since the superelastic and shape-memory effects are optimal and are active at temperatures near body temperature, and also because the material exhibits excellent biocompatibility [1]. Comparisons made between slotted-tube stents made of stainless

steel and those made of Nitinol in rabbit vessels showed that the uncoated stainless steel stents were more thrombogenic and caused more vessel injury than did Nitinol [2].

Using finite element (FE) analysis, the load history of a stent can be simulated. Of interest are load cases that can occur in vivo, as well as those dependent on production technologies; here, the dependence between the material characteristics and the surrounding temperature must be taken into consideration. The conventional calculation procedures and standard characteristic values from linear structural mechanics are no longer applicable. Non-linear FE analysis with constitutive equations adapted to the specific case is indispensable to the simulation of component behavior [3]. The constitutive equations must be experimentally determined for the material being used at the time and its processing status. Experimental testing is essential for validation of the results of FE analysis.

Materials and Methods

Properties of Nitinol

Heat Treatment of Nitinol: To simplify, heat treatment can induce three fundamental effects: separation reactions, recrystalization heating without significant separation, or a combination of these two and diffusion-free structural rearrangements [1]. However, separation reactions require a precipitable alloy.

In a precipitable alloy, nickel-rich compounds (mainly Ni_4Ti_3) begin to diffuse out of the structural matrix once a specific temperature (ca. 300 °C) is reached; this takes the form of grains in the structure. The form and size of these grains, as well as the exact temperatures, are extremely dependent on the composition of the alloy, the prehistory of the material (imperfections, displacement due to strain-hardening), the duration of heat treatment, and the temperature profile [1]. In principle, however, the concentration of nickel in segregated areas leads to less Ni in the lattice structure. This is the reason for the increase in the transformation temperatures with an increase in time or temperature. The segregations that appear are also disruptions in the lattice, comparable to the effects of cold working. The results are increased tensile strength, a reduction in the elongation at fracture, and an influence on the thermal hysteresis. Depending on the alloy, the maximum temperature for this separation process is about 400 – 450 °C. At higher temperatures, the growth of grains is increasingly inhibited, and as the temperature increases further they begin to dissolve. Between 450 °C and 550 °C, both processes are in equilibrium. The alloy remains relatively uninfluenced, even after longer annealing times. However, even in the range between 450 – 550 °C, the recrystalization begins, in which the disrupted points caused by cold work begin to be remedied. The processes that occur in this temperature range can be characterized as combined reactions. At a temperature of 600 °C and a duration of 60 min, a complete homogenization of structure can be expected [1]. At even higher temperatures, the structure finally reaches the starting point as it was solidified from the melt.

The Nitinol is heated using a hollow furnace. A temperature range of 270 °C to 650 °C was chosen in a time interval of 5 min to 60 min, where the focus was placed in the range above 450 °C. In this range, it is possible to set a shape in Nitinol, since the stent blank is laser-cut from a tube smaller than its end diameter. This effect is caused by the beginning recrystalization processes, as well as structural rearrangements.

Determination of Phase Transformation Temperatures: Since most physical characteristics of Nitinol change upon reaching phase transformations (e.g., specific electrical resistance, elastic modulus), each of these changes in the material characteristics, in principle, can be used for a measurement procedure to determine the phase transformation temperature. The procedure used in this study is differential scanning calorimetry (DSC). This procedure determines the latent transformation heat for the phase transformations.

The emphasis here was on the influence of heat treatment on the phase transformation temperatures [4], and the resulting possibility of changing the transformation temperatures (Martensite $\leftrightarrow$ Austenite) [5]. When Nitinol is cooled down from the high-temperature austenitic phase, the martensitic transformation starts and ends at certain temperatures (M_s, martensite start, and M_f, martensite finish, respectively). In a subsequent retransformation different temperatures apply (A_s, austenite start, and A_f, austenite finish, respectively). There is a temperature difference between A_f and M_s that is called temperature hysteresis. For the use of the material as a stent, based on the principle of superelasticity [6], an A_f-temperature significantly below the body temperature should be ensured. In turn, M_f and A_s exert influence on the crimpability of the stent.

To determine the transformation temperatures, small

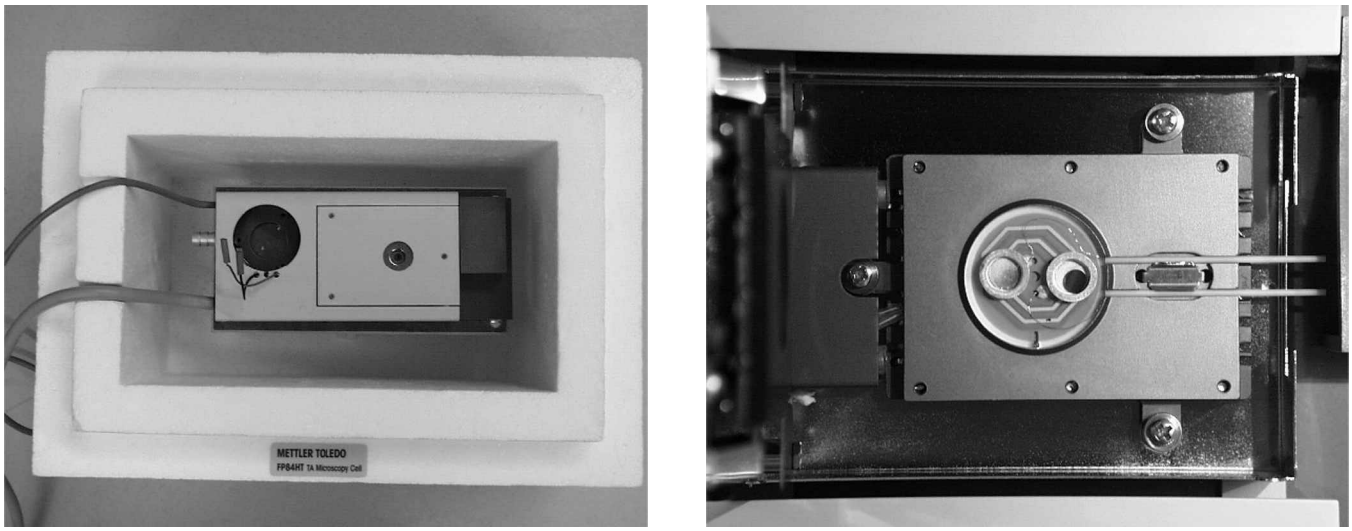

Figure 1. Left: Hot plate in nitrogen reservoir; right: test object (Nitinol) and reference test object (air) in hot plate.

circular discs (D = 3.5 mm) are laser-cut from a Nitinol tube (5 x 0.2 mm; delivery condition) with a total mass of 14 ± 1 mg, and are then heated. A hot plate with DSC function manufactured by Mettler Toledo is used to determine the phase transformation temperatures (Figure 1). The temperature interval between -50 °C and +80 °C was scanned twice for each sample with a heating/cooling rate of 5 K/min. The cooling took place in a nitrogen reservoir containing 5 liters of liquid nitrogen so that environmental temperatures in the area of the hot plate down to -60 °C could be reached.

Mechanical Characteristics of Nitinol: The mechanical characteristics were determined via uni-axial tensile testing with a testing machine manufactured by the company Zwick. For the test objects, "shoulder" bars are cut from the Nitinol tube (5 x 0.24 mm; delivery condition) using a laser (Figure 2). The sample geometry is chosen analogously to the strut-width of the stent in order to judge the influence of thin struts. To determine the hysteresis in the stress-strain diagram, the test objects are cyclically stressed with a deformation speed of 1 mm/min. The first cycle includes the strain of the test object into the superelastic range (8 % strain) with subsequent slackening to 1 MPa. In the second cycle, the test object is then stressed to fracture. The cyclic stress testing is carried out in a temperature equalization chamber at 37 °C.

The Finite Element Procedure

Due to Nitinol's nonlinear material relationships, the conventional calculation procedures and characteristic values, which are derived from linear elasticity theory, are not applicable. In addition, the structure of a stent is generally so complex that analytical calculation results only provide very gross approximations of the actual stress- and strain-status in the stent. To make an exact prediction of the function and lifetime of an implant of this type, as well to optimize these qualities, it is absolutely necessary to obtain an exact knowledge of the mechanical status of the stent in all phases of

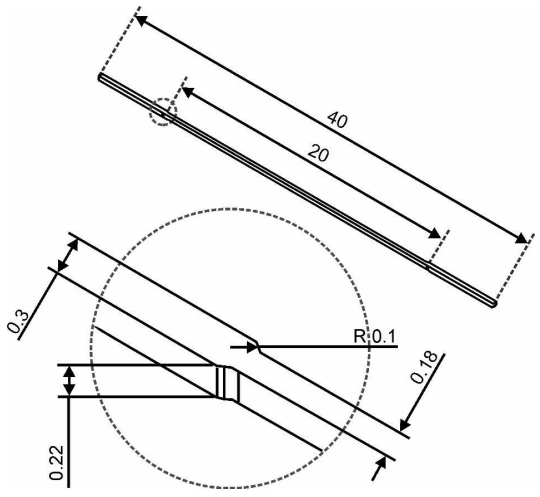

Figure 2. Test object geometry for the cyclic stress test.

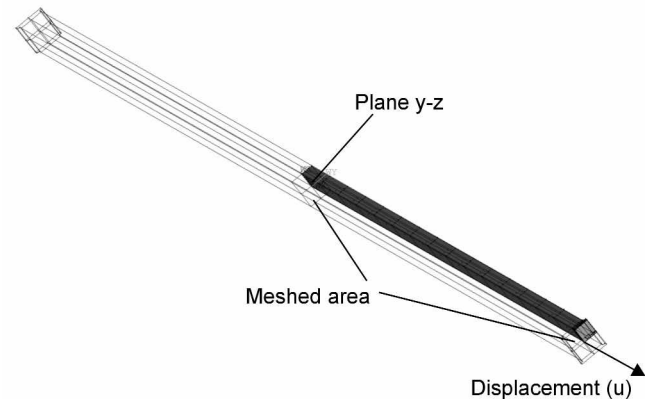

Figure 3. Display of meshed tension test bar with boundary conditions.

use, from expansion to crimping to implantation in the vessel. At this time, the only tool for performing these tasks is the method of numerical simulation (finite element analysis, FEA). The module described in this study is created and calculated using the FEA program ANSYS (ANSYS Inc., USA). The starting point was a parasolid geometry file created with the 3-D volume-modeling system Unigraphics (Unigraphics Solutions Inc., USA), which is imported into the FE system and then meshed. The complete stent geometry is not necessary for FE simulation; appropriate border conditions can be selected in conjunction with the existing symmetries so that the size of the model (number of element) can be reduced. Special attention is paid to the material model, since this is decisive for the predictive capacity of the results. The parameters necessary for this material model are determined in the tension test.

Cyclic load testing for verification of the material model

Cyclic loading of a tension test bar was simulated with FE in order to validate the constitutive equations that were implemented. The calculated results can be directly compared with the experimental results from the tension tests. The dimensions of the model correspond to those of the tension test objects that were used in the experiment. By exploiting all symmetry conditions, the calculation was limited to 1/8 of the geometry. The meshing was carried out with 8-node, solid elements (ANSYS type 45), and is displayed in Figure 3. The total number of elements is 72.

ANSYS does not offer a predefined material model to conduct calculations for shape memory alloys such as Nitinol. Since the program is, however, an open system, the user has various possibilities for constructing an individual model for the material. For this study, it was decided to directly program the recorded representative material behavior (Figure 4) into an ANSYS-input file. The principal procedure is to discretize the material behavior into a finite number of material curves using the austenite and martensite E-modules, as well as the four individual stress-strain pairs A, B, C and D. Via the entry of these values, the material model can be adapted to the given tension test data.

During the calculation, the stress is computed for each element at every iteration step, dependent on the current equivalent stress. Figure 5 shows the material behavior, with a representative curve, that was generated by ANSYS from the input data. The constitutive equations that were found in this way are only the first step toward simulation of the complete material characteristics of Nitinol. A number of simplifications were

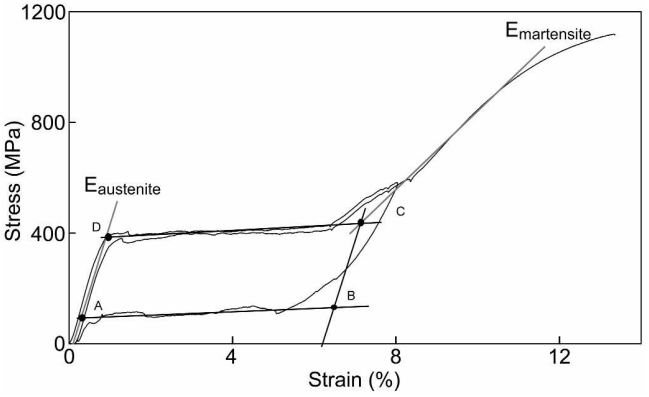

Figure 4. Stress-strain behavior of Nitinol in the tension test.

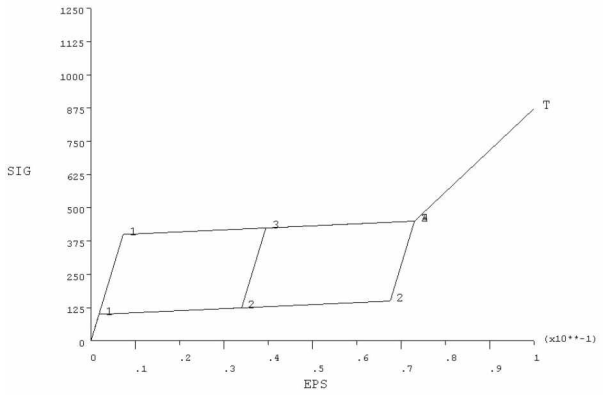

Figure 5. Constitutive equations for the finite element analysis.

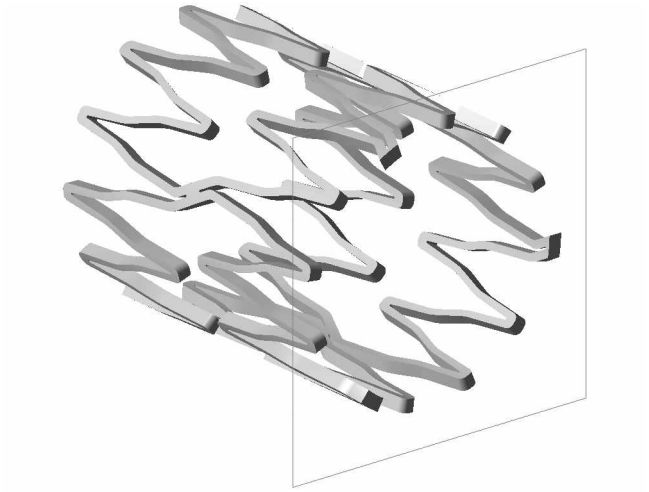

Figure 6. 3-D-display of two ring segments with a plane of symmetry.

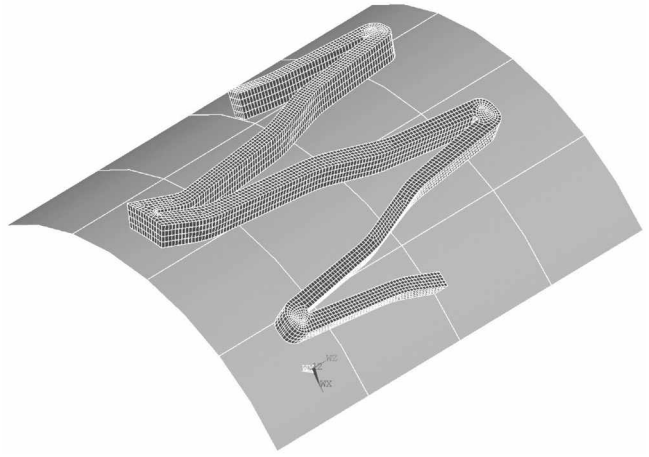

Figure 7. 3-D-display of a calculated stent segment with a membrane.

used, such as neglecting the influence of temperature on the transformation stresses, possible lasting deformations (permanent sets), or significant differences in the tension-compression behavior of the material. Finally, the strain-dependent material assignment to the elements is based on the determination of the equivalent stress or equivalent strain for each element. Whether these assumptions are allowable must be researched further.

Calculation of a Stent Segment: In this study, the FE analyses were limited to the load cases of expansion with subsequent low-strain annealing and crimping. The stent geometry (Figure 6) was created with its actual dimensions using Unigraphics, and imported into ANSYS via the parasolid interface. The smallest repeating element of the structure was determined and meshed with solid elements of ANSYS type 45 (Figure 7). Mesh refinements were undertaken in areas where the strain gradients were expected to be higher, such as at branchings in the structure. Due to the consistent utilization of the repeating symmetric structure, the number of elements in the model could be kept to 15530, which is an acceptable range.

Results and Discussion

Determination of Transformation Temperatures

DSC analyses were performed to determine the transformation temperatures. From the graphs, only the characteristics A_f (austenite finish) and A_s (austenite start) could be determined and evaluated with certainty. Figure 8 displays examples of the regions of interest for determination of the characteristic values A_f and A_s for a heat-treated Nitinol test object.

The curves displayed in Figure 9 show sample progressions of the A_f- and A_s-temperatures as a function of the annealing temperature for two different annealing times. In the range where the A_f- and A_s-temperatures are increasing, the nickel-rich composites diffuse out of the matrix, which is accompanied by segregation into nickel grains. The time-dependency becomes smaller and smaller at higher temperatures, which is a further indication for diffusion as the cause of this effect, since diffusion processes are time-dependent. Temperatures above the turning point lead to dissolution of the nickel grains, and the alloy becomes increasingly homogenized until the grains reach their transformation temperature determined from the melt. In order to examine the transformation range at the turning point in Figure 9 even more closely, additional annealing times were researched in the indicated region of interest. As shown in Figure 10, there was a strong temperature dependence for very short annealing times.

Mechanical Characteristics of Nitinol

In Figure 11, the stress-strain behavior of a representative heat-treated Nitinol test object under cyclic stress is displayed. In addition, the characteristic points for the upper and lower plateaus are shown, as well as the E-modules $E_{austenite}$ and $E_{martensite}$. With the characteristic points, the characteristic values for UPS (upper plateau

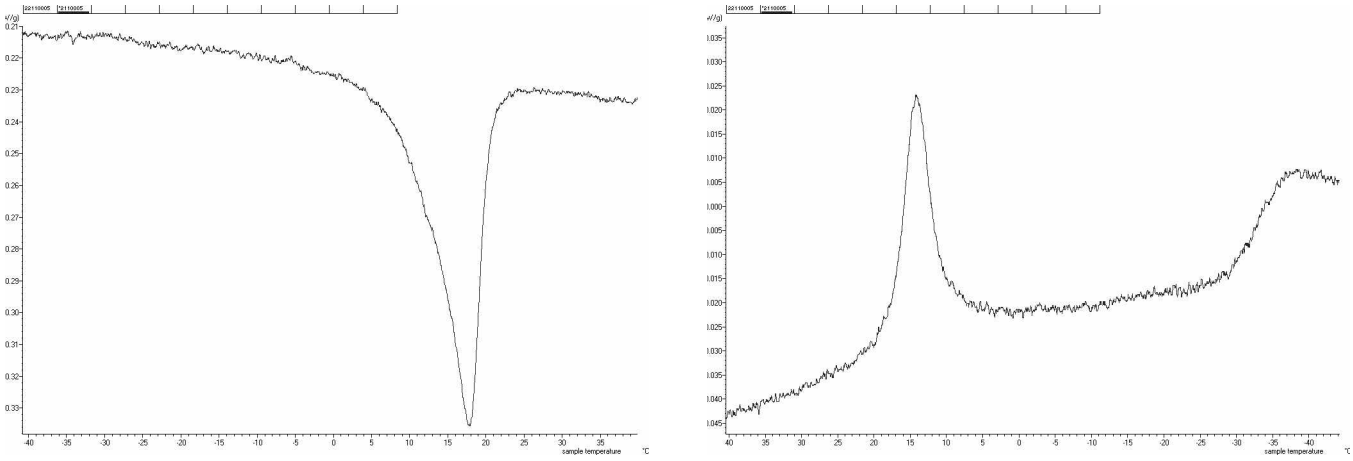

Figure 8. Phase transformation for a heat-treated test object made of Nitinol; left: detail of annealing curve; right: detail of cooling curve.

stress) and LPS (lower plateau stress) can be derived as averages from the stresses at points 1 and 2.

Figure 12 depicts the variation of the upper plateau stress as a function of temperature and heat-treatment duration. The heat treatment generally causes the plateau to sink by about 100 MPa with reference to the starting material. Dependence on the annealing temperature is not significant. Figure 13 shows the length of the plateau for different heat treatments. Comparing this with Figure 9, it is clear that maximal transformation temperatures correspond to a minimum of superelasticity. The segregations that are most frequent at this annealing temperature operate as additional sources of structural disruption, which inhibits the formation and spread of martensitic structure. At higher temperatures, the length of the plateau increases significantly, which can be explained by the dissolution of the nickel deposits and by the recrystalization effects.

Finite Element Modeling

In order to assess the design of the stent, in a first approximation the following stress cases were simulated using a 3-D model:

- Expansion of the stent to the nominal diameter,
- Stress-free annealing,
- Crimping of the stent at the internal diameter of the delivery device.

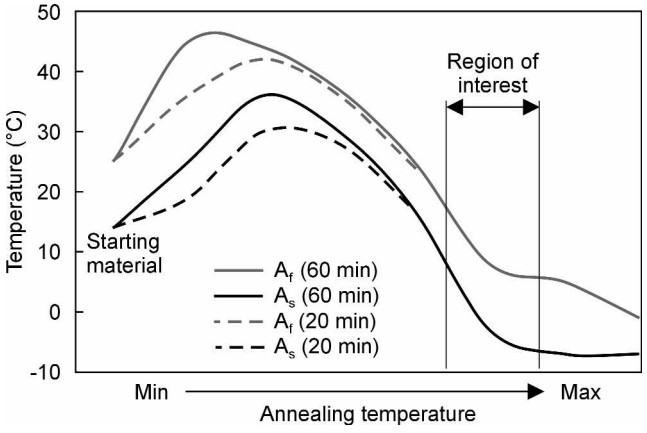

Figure 9. A_s (austenite start) and A_f (austenite end) as a function of annealing times (20 min and 60 min).

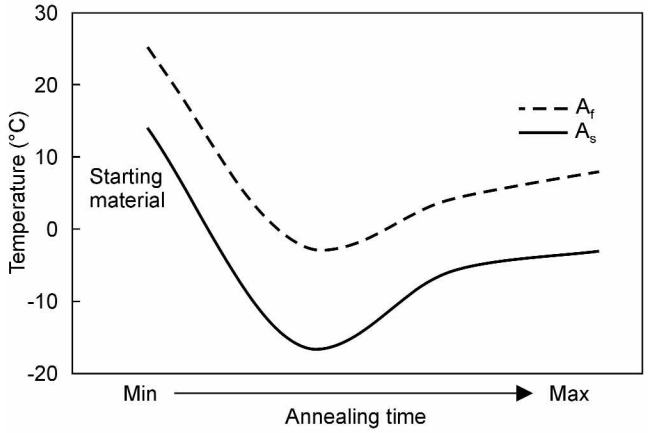

Figure 10. Dependence of A_s (austenite start) and A_f (austenite end) temperatures on the annealing time at a constant annealing temperature.

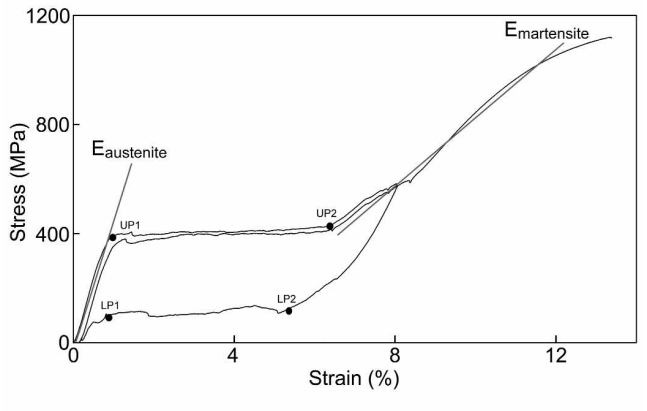

Figure 11. Stress-strain behavior of a representative heat-treated stress test object under cyclic load.

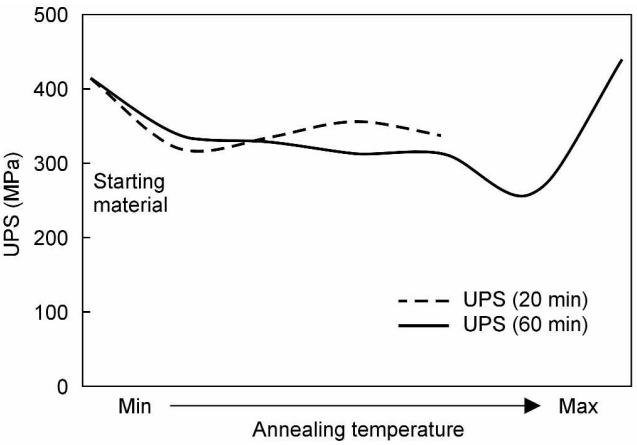

Figure 12. Upper plateau stress UPS as a function of the temperature and the annealing time.

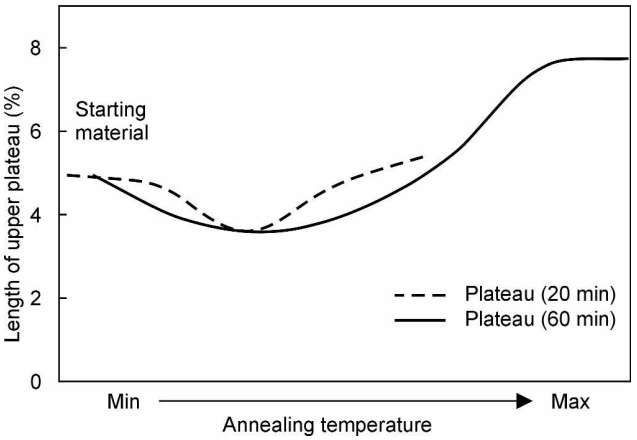

Figure 13. Length of the upper plateau as a function of the heat-treatment factors.

These calculations offer the developer important constructive information regarding maximum strains and stresses in the individual stress steps. The stent geometry can then be modified and optimized both quickly and efficiently. Calculating a 2-D model of stent deployment can also be performed for an initial estimation. However, for complex stent geometries, it must be considered that the calculations carry no predictive weight regarding, e.g., counterrotations of individual segment rings or the protrusion of individual struts during the expansion and crimping processes.

Validation of the Constitutive Equations

In order to validate the self-formulated constitutive equations, the force- and displacement data were determined for the nodal point where the load was applied. The data were then converted into a stress-strain diagram (Figure 14) in order to make them easier to compare. No differences were found between this curve and the formulated material curve.

Strain and Stress After Expansion

One of the possible production steps is to cut the stent structure into a small tube using a laser, and then to expand the tube to its significantly larger nominal diameter. Then, the material is subjected to a special heat treatment that leaves the material in a stress-free state, in order to set the stent shape at the nominal diameter [7]. The maximum stresses and strains are monitored so that the production process does not lead to component failure. The maximum stress and strain are shown in Figure 15 and Figure 16 for a representative expansion diameter. All calculated values were within the superelastic range, and thus far below the elongation at rupture.

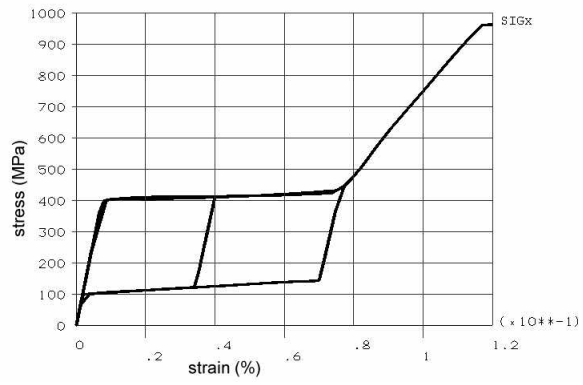

Figure 14. Stress-strain curve for the nodal point where the load was applied.

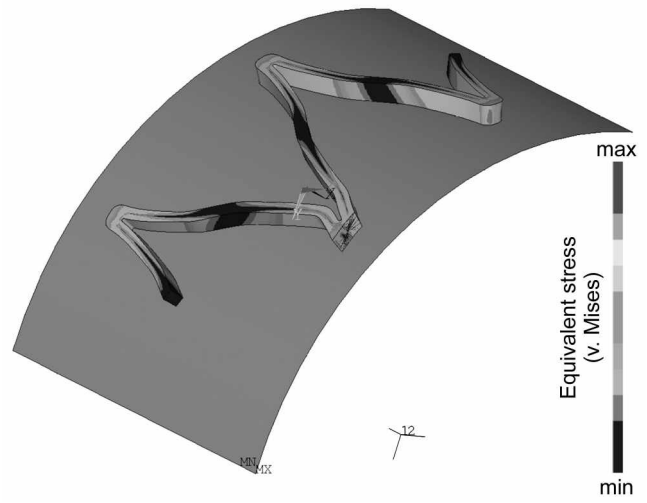

Figure 15. Depiction of the equivalent stress as per v. Mises after the expansion of a stent segment.

Figure 16. Depiction of equivalent strain as per v. Mises after the expansion of a stent segment.

Strain and Stress After Crimping

Crimping is the radial compression of the stent to a diameter that is as small as possible in order to load the stent onto the delivery system. This procedure preferably occurs at temperatures below A_s, since at this temperature, pseudoplastic displacements of the martensite lattice occur that, upon heating above A_f, completely degenerate due to transformation into austenite. For the FE-simulation of this load-step, all stresses from the previous load-step are set to zero, so that only the deformed shape displaying the nominal diameter remains. This is the equivalent of stress-free annealing.

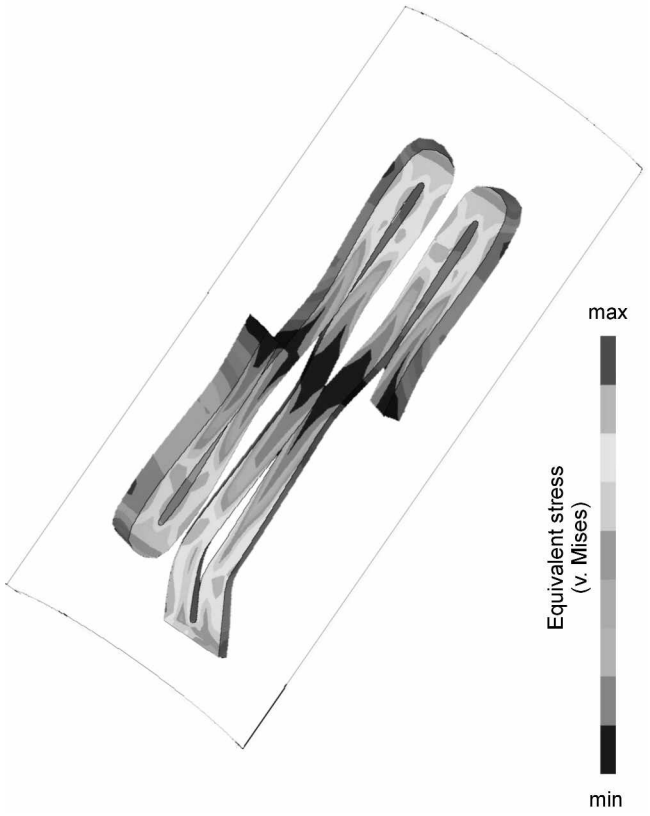

Figure 17. Display of equivalent stress as per v. Mises after the crimping process of a stent segment.

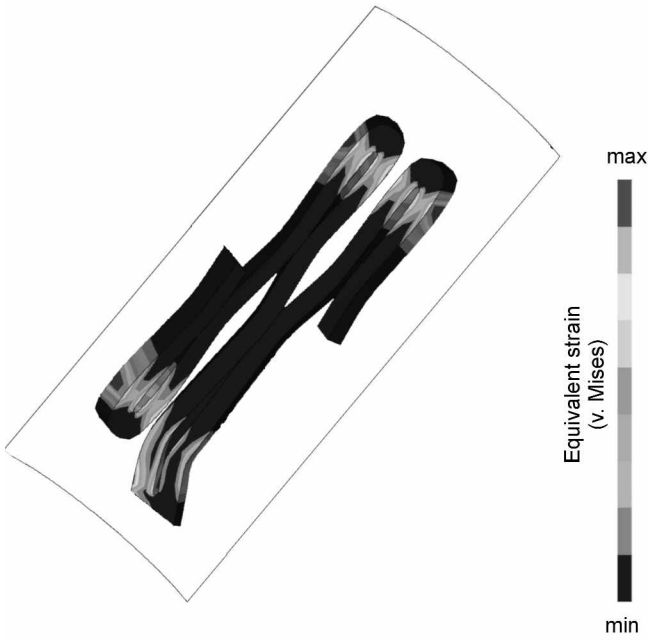

Figure 18. Display of equivalent strain as per v. Mises after the crimping process of a stent segment.

Then, the stent segment is radially compressed via contact formulation. The strains and stresses that result for this status are displayed in Figure 17 and Figure 18. As with the expansion process, no values outside of the superelastic range were recorded.

Conclusion

From the parameter studies that were carried out, an optimal heat treatment was able to be found for the application of the material Nitinol as an implant material. The parameters are not very time-critical, and guarantee secure form setting. The A_f-temperature after heat treatment of the material lies significantly below the temperature at which the material is used (37 °C body temperature), ensuring optimal stent mechanical characteristics and full functionality in vivo. For A_f, a range of about 15 – 25 °C is viewed as ideal. If A_f is higher, then in some cases the austenite transformation might not be complete, and the stent no longer expands entirely in the vessel, and does not reach is maximum strength (collapse pressure). At a lower A_f, the "permanent set" (superelastic window) and the plateau stresses are higher, which is especially disadvantageous for the lower plateau (higher forces upon release, higher pressure of stent against vessel wall). It must be attempted to maximize the plateau length (about 7 %) in order to achieve maximum one-way effects.

Difficulties such as obtaining and inputting a characteristic material curve for the microstructure of the individual struts of a stent, the construction of a material model with consideration of hysteresis, as well as modeling the crimping geometry through reliable contact calculation were able to be overcome. In addition, it was shown that the constitutive equations that were obtained experimentally could be implemented in an FEA system. Further research must be conducted regarding the allowability of the assumptions that were made; these included the neglect of both the temperature and the differences in compression-tension behavior.

In addition, failure analyses of stent structures made of Nitinol, conducted with FEA, are also necessary with respect to product approval as per EN 12006-3. Loss criteria must then be formulated that offer a more extensive load history of the stent; these can include deployment, vessel anatomy, and physiology. These will be integrated into the stent design as construction requirements. The FE analysis is an extremely important tool in the development of a materials-optimized stent design. The results should, however, always be validated with data that are obtained experimentally with stent test objects.

Acknowledgement

We thank the company CAD-FEM (Berlin, Germany) for their generous support in creating models and converting the experimental data into implementable constitutive equations for finite element analysis via ANSYS.

References

[1] Treppmann. Thermomechanische Behandlung von NiTi. In: Fortschrittberichte VDI, Reihe 5: Grund- und Werkstoffe No. 462. Düsseldorf: VDI-Verlag. 1997.

[2] Sheth S, Litvack F, Fishbein MC, et al. Subacute thrombosis and vascular injury resulting from slotted-tube Nitinol and stainless steel stents in rabbit carotid artery model. Circulation. 1996; 94: 1733-1740.

[3] Duerig TW, Pelton AR, Stöckel D, et al. In: Duerig TW. Engineering Aspects of Shape Memory Alloys. London: Butterworth-Heinemann. 1990.

[4] Bataillard L, Gotthardt R. Influence of Thermal Treatment on the Appearance of a Three Step Martensitic Transformation in NiTi. Journal de Physique IV. 1995; 5: 647-652.

[5] Pelton AR, DiCello J, Miyazaki S. Optimization of processing and properties of medical grade Nitinol wire. Min Invas Ther & Allied Technol. 2000; 9:107-118.

[6] Duerig TW, Pelton AR, Stöckel D. The use of superelasticity in medicine. Metalle. 1996; 9: 569-574.

[7] Rebelo N, Walker N, Foadian H: Simulation of implantable Nitinol stents. ABAQUS Users' Conference. 2001: 1-14.

Contact
K. Koop
Institut für Implantat-Technologie
Friedrich-Barnewitz-Strasse 4
D-18119 Rostock-Warnemünde
Germany
Telephone: +49 381 66 09 413
Fax: +49 381 66 09 400